Homodimerization of the G protein SRβ in the nucleotide-free state involves proline cis/trans isomerization in the switch II region

Thomas U. Schwartz*†‡, Daniel Schmidt†§, Stephen G. Brohawn*§, and Günter Blobel†‡

*Department of Biology, Massachusetts Institute of Technology, 77 Massachusetts Avenue, Cambridge, MA 02139; and †Howard Hughes Medical Institute, Laboratory of Cell Biology, The Rockefeller University, 1230 York Avenue, New York, NY 10021

Contributed by Günter Blobel, March 19, 2006

Protein translocation across and insertion into membranes is essential to all life forms. Signal peptide-bearing nascent polypeptide chains emerging from the ribosome are first sampled by the signal-recognition particle (SRP), then targeted to the membrane via the SRP receptor (SR), and, finally, transferred to the protein-conducting channel. In eukaryotes, this process is tightly controlled by the concerted action of three G proteins, the 54-kD subunit of SRP and the α- and β-subunits of SR. We have determined the 2.2-Å crystal structure of the nucleotide-free SRβ domain. Unexpectedly, the structure is a homodimer with a highly intertwined interface made up of residues from the switch regions of the G domain. The remodeling of the switch regions does not resemble any of the known G protein switch mechanisms. Biochemical analysis confirms homodimerization *in vitro*, which is incompatible with SRα binding. The switch mechanism involves cis/trans isomerization of a strictly conserved proline, potentially implying a new layer of regulation of cotranslational transport.

cotranslational transport | proline isomerization | signal-recognition particle receptor

Nascent proteins, destined for secretion or membrane insertion, are first targeted to the endoplasmic reticulum (ER) in eukaryotes or the plasma membrane in bacteria. Targeting in eukaryotes occurs primarily via the conserved signal-recognition particle (SRP) pathway (1). This cyclic pathway starts with SRP, a ribonucleoprotein complex consisting of the 300-nucleotide SRP-RNA and six proteins, recognizing a ribosome-nascent chain (RNC) complex and arresting translation. In a second step, the stalled SRP–RNC complex docks with the ER membrane-bound SRP receptor (SR) (2, 3), which is dynamically associated with the protein-conducting channel (PCC or Sec61 complex) (4). Third, the RNC is detached from the SRP, binds to the PCC, and releases the nascent polypeptide chain into an aqueous pore in the channel (5, 6). Protein synthesis can then continue. Concomitantly, SRP and SR dissociate, ready for a new cycle of protein targeting. GTP binding and hydrolysis by three synchronized G proteins regulate the process and ensure unidirectionality (7, 8).

Intense investigation of the protein targeting process by x-ray crystallography and cryoelectron microscopy has lead to the structural characterization of domains and interactions (9, 10). As a result of these advances, several key steps are now relatively well understood. The recent cryoelectron microscopic structure of the SRP–RNC complex shows how the elongated SRP wraps around the large ribosomal subunit, binding the N-terminal signal sequence of the nascent chain at the exit tunnel via SRP54 at one end of the molecule and arresting translation by blocking the elongation-factor-binding site with its other end (11). SRP54, the only SRP protein with a bacterial homologue, has two functional domains; the C-terminal M domain is the signal sequence-binding interface, and the N-terminal composite NG domain has regulatory GTPase activity. Signal sequence binding by SRP54 results in increased GTP affinity. GTP binding, in turn, allows stable association with the SRP receptor, harboring a structurally similar NG domain at the C terminus of its α subunit. The two NG domains form a quasi-2-fold symmetrical engagement complex with a composite active site containing two GTP molecules. The recent elucidation of the crystal structure of this complex beautifully explains the tight coupling of SRP–SR association and subsequent dissociation upon GTP hydrolysis (12, 13). Disengagement of SRP from SR and RNC is directly linked to the docking of the RNC to the PCC. PCC and SRP binding to the RNC are mutually exclusive (11, 14).

Whereas bacteria appear to solely use homologues of SRP54 (Ffh) and SRα (FtsY) for regulation of cotranslational protein targeting, eukaryotes have developed another layer of regulation that is far less well understood. This regulation involves the β-subunit of the SR, which is unique to eukaryotes. SRβ consists of an N-terminal transmembrane helix and an Arf-like G domain (15, 16). The transmembrane helix anchors the receptor in the ER membrane, although severing that helix does not entirely compromise function (17). The crystal structure of yeast SRβ in complex with the interaction domain SRX of SRα revealed that the two subunits assemble only when SRβ is GTP-bound, analogous to all other structurally studied G protein–effector complexes (16). Thus, SRβ regulates the assembly of SR. To more fully describe the switch cycle of SRβ, we now report the structure of nucleotide-free SRβ. This structure reveals an unprecedented G protein switching mechanism involving homodimerization of SRβ controlled by proline isomerization.

Results

Structure of SRβ. Attempts to crystallize SRβ from *Saccharomyces cerevisiae* (residues 31–244), with the N-terminal transmembrane helix truncated, initially failed because of solubility problems. We then constructed a circularly permuted variant [termed $SR\beta_{D210K183}$ (18), here referred to as cpSRβ for simplicity] that had increased solubility as well as stability and that crystallized. In this cpSRβ construct, the spatially close terminal residues 31 and 244 are joined with a heptapeptide, and the long flexible region between helix α4 and strand β6 is removed (Fig. 1). The engineered domain was properly folded and fully functional, as judged by GTP-dependent binding to SRα (18). Crystals of nucleotide-free cpSRβ grew in space group $P6_1$, with two molecules in the asymmetric unit. The structure was solved by molecular replacement with SRβ from the SRβ-GTP–SRX

Conflict of interest statement: No conflicts declared.

Abbreviations: ER, endoplasmic reticulum; PCC, protein-conducting channel; RNC, ribosome-nascent chain; SR, SRP receptor; SRP, signal-recognition particle.

Data deposition: The atomic coordinates have been deposited in the Protein Data Bank, www.pdb.org (PDB ID code 2GED).

§D.S. and S.G.B. contributed equally to this work.

‡To whom correspondence may be addressed. E-mail: tus@mit.edu or blobel@rockefeller.edu.

BIOCHEMISTRY

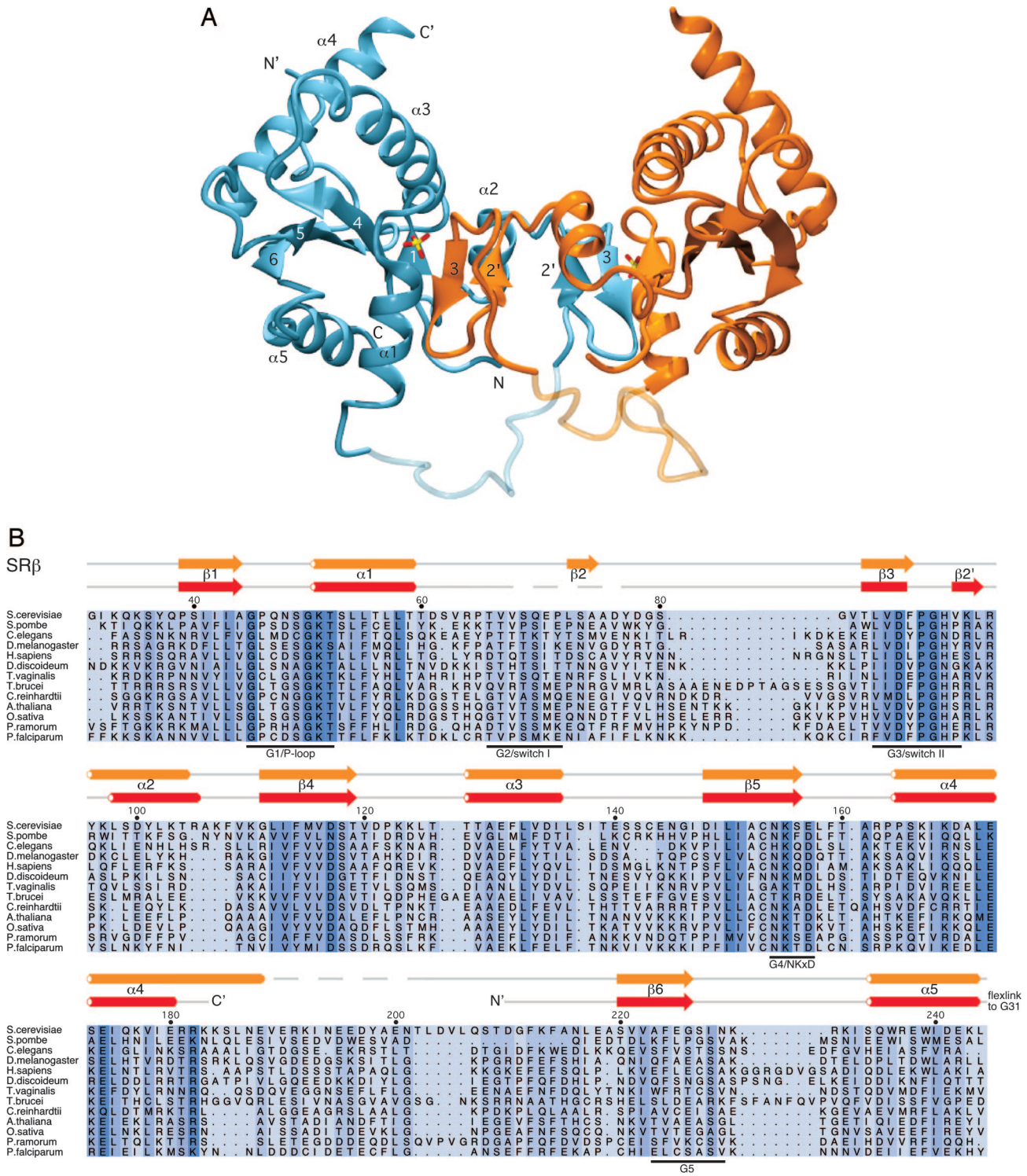

Fig. 1. Structure of the cpSRβ homodimer and sequence alignment. (*A*) Two molecules of cpSRβ (blue and orange) assemble around a vertical twofold axis. Secondary structure elements are labeled. The disordered part of the switch region is half-transparent. A sulfate ion occupies the β-phosphate position of the nucleotide-binding site. N′ and C′ designate the termini of the circularly permuted protein construct used for crystallization. (*B*) Sequence alignment of SRβ orthologues. Sequence conservation is shown in a blue gradient. Secondary structure elements of SRβ-GTP (PDB code 1NRJ) and this structure are shown above the sequence in orange and red, respectively. Dashed lines indicate disordered regions. Nucleotide-binding motifs are labeled below the sequence.

complex as the starting model (see Table 1, which is published as supporting information on the PNAS web site). The 2.2-Å crystal structure of nucleotide-free cpSRβ is very similar to SRβ-GTP bound to SRX, except for the switch residues 61–101 (Fig. 1). Both cpSRβ molecules superimpose well with a rms deviation of 0.21 Å comparing 155 Cα atoms. In the nucleotide-binding site, a sulfate ion is bound in the position that is usually occupied by the β-phosphate of the nucleotide (see Fig. 4, which is published as supporting information on the PNAS web site). The β-phosphate is the main contributor to nucleotide affinity

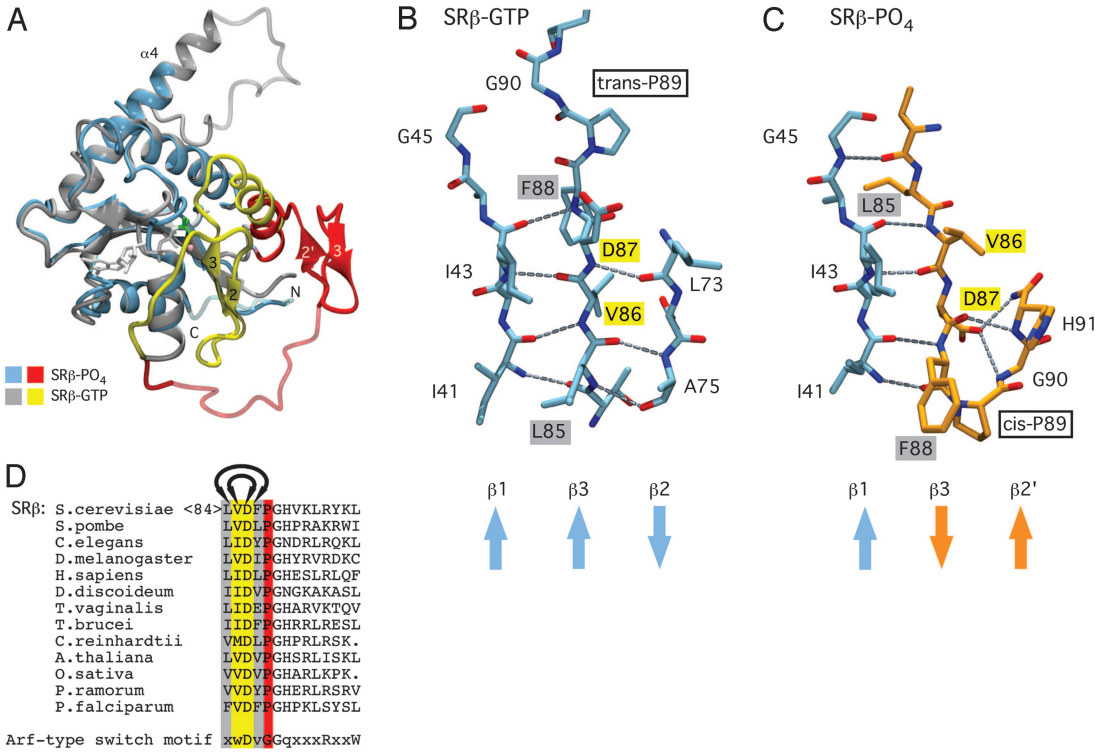

Fig. 2. Details of the SRβ switch positions. (*A*) Superposition of the two switch positions of SRβ.The GTP molecule is in white, and the leaving group (γ-phosphate) is in green. (*B* and *C*) Atomic detail of the environment of strand β3 in the GTP form (*B*) and the nucleotide-free form (*C*). In the dimeric nucleotide-free form, an antiparallel β-sheet is formed in trans between strands β1 and β3 of the neighboring molecules (carbon atoms blue and orange, respectively). In the monomeric GTP form, the β-sheet is parallel and in cis. Strand β3 is flipped with respect to β1; positions 85/88 (gray boxes) and 86/87 (yellow boxes) switch positions as a result. Proline 89 changes its conformation from cis to trans going from the nucleotide-free form to the GTP form. (*D*) Sequence comparison of the β3 region with the Arf-type switch motif. Arf-type G proteins are the closest structural homologues to SRβ, sharing very similar GTP forms. The GDP form of Arf-type and the nucleotide-free form of SRβ differ significantly, which can be explained by the distinct sequence-conservation patterns. The residues changing positions in the SRβ switch are indicated with arrows; the strictly conserved proline (glycine in Arf) is in red.

in small G proteins (19). A sulfate ion bound in the β-phosphate position has been observed in other P-loop protein structures (20–22). In the eukaryotic cell, the β-phosphate position of dimeric SRβ is probably occupied by inorganic phosphate, the intracellular concentration of which is $\approx$2 mM (23).

In contrast to earlier suggestions (16), the extended helix α4 does not change its orientation as part of the observed switch. In both copies of SRβ in this homodimeric structure, the helix α4 points outward from the protein core in exactly the same way as seen in SRβ-GTP (Fig. 2*A*).

Switch Mechanism. Two cpSRβ molecules form a face-to-face homodimer centered around a 2-fold axis. The dimer interface is composed of identical residues from each monomer, burying a total surface area of 2,982 Å^2 from the solvent. Compared with SRβ-GTP, the switch region is completely remodeled, unrelated to any known G protein switch mechanism. Because of the absence of a phosphate in the GTP γ-position in the nucleotide-binding site, switch I (residues 61–72) has lost its anchoring point and adopts a flexible conformation, with most of its residues invisible in the structure. Interswitch (residues 73–87) and switch II (residues 88–101) rotate away from the protein core to allow interaction with the second SRβ molecule. The interswitch β-hairpin (comprising β2 and β3) unzips from β1 in the protein core, and β3 reanneals in trans with β1 of the other molecule. Remarkably, whereas β1 and β3 form a parallel β-sheet in SRβ-GTP, they are antiparallel in this structure (Fig. 2 *B* and *C*; and see Movie 1, which is published as supporting information on the PNAS web site). Furthermore, the first turn of helix α2 of switch II unwinds and forms the new strand β2′ that pairs in cis with β3, replacing β2. Maybe most notable in this switch conformation is proline 89, which is part of the tight turn between β3 and β2′ (Fig. 2*C*). Here, proline 89 adopts the cis conformation, as opposed to the trans conformation seen in the GTP-bound SRβ structure.

Quasidomain Swapping. The cpSRβ homodimer structure resembles domain-swapped dimers, that is, subdomains are exchanged between identical partners (24, 25). Bona fide domain swapping is defined such that, aside from the oligomer, a closed monomeric form of the protein also exists. In all cases studied, the hinge regions connecting the swapped domain to the core domain are flexible, and this flexibility is required to allow for switching. Also, the swapped domain usually resides at either terminus of the protein (24, 25). Only a few proteins are known to swap a central element. In the blood coagulant factor IX/X-bp, internal loops are swapped (26). In the cyclophilin Asp f 11, two neighboring strands of a central five-stranded β-sheet are swapped between two subunits (27). Homologous, monomeric structures of Asp f 11 are known, adopting exactly the same conformation as their nonswapped structure. Regarding SRβ, the existence of a closed monomeric, nucleotide-free form appears unlikely. One of the two hinges (residues 94–96) connecting the swapped domain to the rest of the protein is well ordered and an integral part of the homodimer interface (see Fig. 5, which is published as supporting information on the PNAS web site). In fact, residues arginine 95 and tyrosine 96 form a short antiparallel intermolecular β-sheet. Remodeling in this area to conceive a potential closed monomeric form would result in an at least locally reshaped molecule.

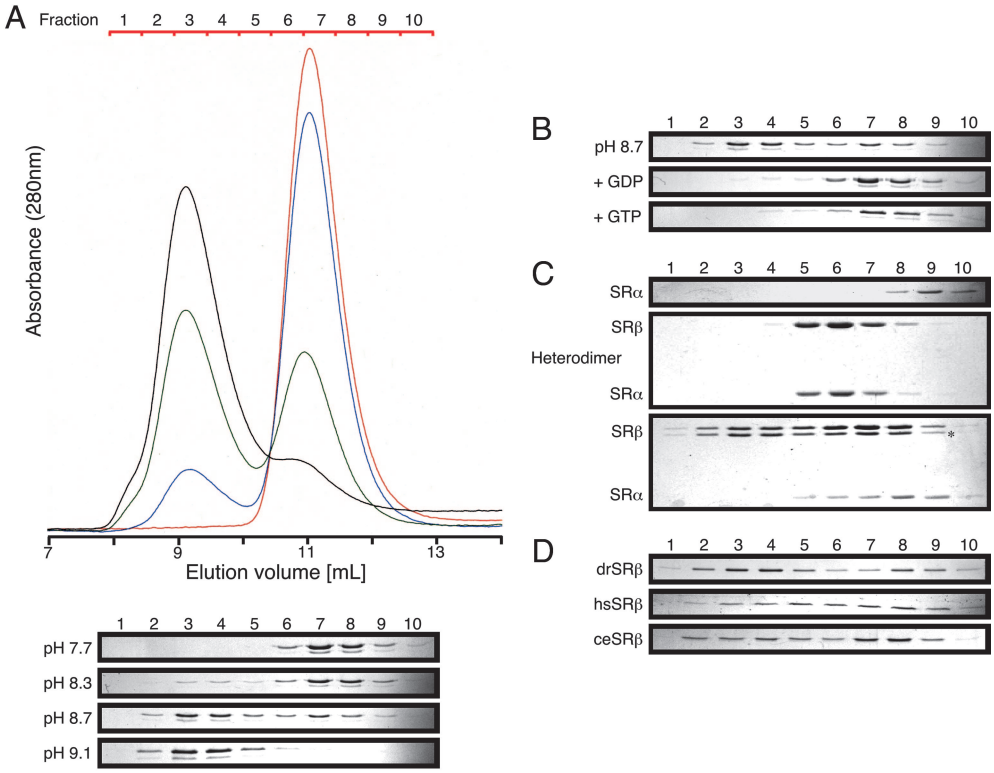

Fig. 3. Biochemical evidence for dimerization of SRβ *in vitro*. (*A*) SRβ dimerization can be demonstrated *in vitro* and is pH-dependent. Nucleotide-free, initially monomeric SRβ was incubated for 6 days at 4°C and assayed for dimer formation by gel filtration. Elution profiles for SRβ incubated at pH 7.7 (red), 8.3 (blue), 8.7 (green), and 9.1 (black) are shown. SRβ in eluted fractions was analyzed by SDS/PAGE. (*B–D*) SDS/PAGE analysis of gel-filtration fractions collected as in *A*. (*B*) Nucleotide-bound SRβ does not dimerize *in vitro*. SRβ was incubated at pH 8.7 alone and with GDP or GTP for 6 days before gel-filtration analysis. (*C*) SRβ homodimer does not bind SRα. Profiles of SRX (SRα_{1-158}), SRβ-GTP/SRX heterodimer, and SRβ homodimer/monomer incubated with SRX are shown. *, appearance of an SRβ doublet on SDS/PAGE gels is due to partial C-terminal degradation of the protein during purification. (*D*) Dimerization of SRβ from *D. rerio*, *H. sapiens*, and *C. elegans* can also be demonstrated *in vitro*. SRβ from the three different organisms was incubated at pH 8.7 at 4°C for 2, 8, and 11 days, respectively, before gel filtration.

The Sequence Signature of the SRβ Switch. Dimerization often occurs in crystal structures. The question arises whether such dimers are merely the result of fortuitous crystal packing or whether they are physiologically relevant. For SRβ, there is no published data on its oligomeric state in the cell. The structure and additional biochemical data suggest, however, that dimerization is likely to occur *in vivo*. First, SRβ is membrane-bound via its N-terminal transmembrane helix, missing in this structure. In the cpSRβ dimer structure, the domain pair is arranged such that the N termini of both monomers are on the same side of the molecule, consistent with the fact that both transmembrane helices have to be anchored to the membrane. Second, the dimer interface is much larger (2,982 Å^2) and more elaborate than a typical crystal packing interface (28). Aside from these circumstantial facts, amino acid sequence comparison of SRβ orthologues strongly indicates that homodimerization is functionally conserved. Regarding the interface, the most restrained area is the stretch of residues 85–89 (Fig. 2*D*). Proline 89, which undergoes cis/trans isomerization as part of this G protein switch, is strictly conserved. Residues 85–88 form strand β3, which hydrogen-bonds β1 either in parallel (GTP form) or antiparallel fashion. As a result of this flip of β3, amino acids 85 and 88 and residues 86 and 87 exchange positions. To do so, the side chains of these residue pairs have to match in size to avoid steric clashes. This subtle, nonetheless crucial, requirement is phylogenetically well conserved in all SRβ orthologues (Fig. 2*D*). Interestingly, however, this sequence pattern is not conserved in the Arf-type G proteins, which are, otherwise, the closest relatives of SRβ. There, the proline 89 position is strictly conserved as glycine, and the residue pairs equivalent to positions 86/87 and 85/88 in SRβ are not conserved to match in size.

Although the indications are strong that the observed dimeric SRβ is physiologically relevant, we set out to test this hypothesis biochemically.

SRβ Homodimerization *in Vitro*. Judged by gel filtration, we could hardly observe dimer formation in freshly made SRβ preparations. Recombinant *S. cerevisiae* SRβ is predominantly GTP-bound when isolated from *Escherichia coli* extracts (29). To study homodimerization *in vitro*, SRβ was first purified to homogeneity in monomeric, nucleotide-free form in phosphate buffer. The protein was then incubated at 4°C without nucleotide or in the presence of either GDP or GTP. In a strongly pH-dependent manner, homodimerization was observed after several days of incubation. Whereas essentially no dimer formation was observed at pH 7.7, a majority of SRβ was dimerized at pH 9.1 after 6 days (Fig. 3*A*). Further incubation did not significantly change the chromatograms, except for slow accumulation of aggregated protein (data not shown). Thus, after 6 days, a pH-dependent equilibrium between monomeric and dimeric SRβ is observed. The very slow dimerization kinetics are probably due to the isomerization of proline 89, which has a high transition-state energy barrier (14–24 kcal/mol). Dimer formation is inhibited when SRβ is GDP- or GTP-bound (Fig. 3*B*). Next, homodimerized SRβ was assayed for interaction with SRX, the interaction domain of SRα (Fig. 3*C*). For this purpose, nucleotide-free, partially homodimerized SRβ was incubated with SRX and complex formation analyzed by gel filtration. As expected from

the structure in which the SRX interaction surface is no longer accessible, no SRX is found in complex with homodimerized SRβ. Some of SRX is weakly bound to monomeric SRβ, similar to the result published with GDP-bound SRβ (16). The observation that SRX cannot bind homodimerized SRβ in the assay suggests that the dimer formed *in vitro* and in the crystal are very similar.

As described above, SRβ has a distinct sequence-conservation pattern in the switch II region that is different from its closest relatives, the Arf-type G proteins. Although the switch II sequence conservation reflects the requirements for the transition from the GTP-bound to the nucleotide-free state, site-directed mutagenesis to disrupt the transition is not straightforward. Unlike a typical dimer interaction surface, most residues involved have a dual role, in that they are also critically important for the stability of the protein or nucleotide binding. Still, a mutation intended to sterically disrupt the dimer surface (V86W) and one designed to make peptide-bond isomerization energetically less favorable (P89A) resulted in soluble, functional scSRβ. However, both mutants dimerized *in vitro* similarly to wild-type SRβ (data not shown). Presumably, the total dimerization interface area is large enough to tolerate the single amino acid changes, and the *cis*-peptide bond configuration in P89A was retained. This retention is not completely unexpected and has been observed in several other cases (30, 31). To verify SRβ-specific homodimerization, we performed the gel-filtration assay with SRβ from three additional organisms: *Drosophila melanogaster*, *Caenorhabditis elegans*, and *Homo sapiens*. In all cases, homodimerization was observed (Fig. 3*D*), with moderately different kinetics compared with scSRβ. This experiment strongly supports the evolutionary conservation of this conformational switch.

Discussion

The structure of the nucleotide-free cpSRβ domain unveils, together with the previously known structure of SRβ-GTP–SRX, snapshots of the switch mechanism of this G protein. This type of remodeling of a switch region is unprecedented. In the small G proteins studied so far, a number of different switch modes have been observed that are correlated with the diverse functions of the respective proteins (32). SRβ has a singular role in cotranslational targeting and is not part of a larger family of orthologues (33). Therefore, it is rather likely that the SRβ switch mechanism is unique.

What might be the role of homodimerization? The structural and biochemical data indicate that homodimerized SRβ is unable to interact with SRα; therefore, a functional receptor cannot be assembled, and cotranslational transport would halt. The eukaryotic cell has developed an elaborate system to rid the ER of misfolded secretory proteins by transporting them back into the cytosol, where they are degraded (34, 35). In such a situation of ER stress, further import of secretory proteins is undesirable, and SRβ could act here as a regulator. Similarly, in slow-growing or stationary cells, SRβ could be held in a dormant state by homodimerization, stopping protein translocation. It is interesting to note that Toc34, the G protein that is considered to function similarly to SRβ in the regulation of protein import into chloroplasts (36), dimerizes in its GDP form (37, 38), perhaps reflecting an evolutionary conserved function.

Proline switching adds another layer of regulation to SRβ. So far, the role of proline isomers is widely recognized in connection with protein folding, and, in most folded proteins, the isomer is fixed (39, 40). However, the role of proline as a means for conformational switching is starting to emerge (39, 40). *In vitro*, proline isomerization of SRβ is slow, presumably because it is uncatalyzed. Thus, it appears likely that a yet-to-be-identified peptidyl-prolyl cis/trans isomerase may act on SRβ in the living cell and also suggests that SRβ would not switch into the nucleotide-free homodimerized state in every translocation cycle. Using isothermal calorimetry, we measured a nucleotide affinity for monomeric SRβ of 2 ± 1 μM for GTP and 8 ± 3 μM for GDP in a buffer containing 10 mM potassium phosphate (see Fig. 6, which is published as supporting information on the PNAS web site). In the cell, the concentration of GTP and GDP is reported to be 923 and 128 μM, respectively (41). Thus, monomeric SRβ would normally be nucleotide-bound. The last protein targeting step is the transfer of the nascent polypeptide chain from the SRP to the PCC. This step requires all three regulatory G proteins involved in the process to hydrolyze GTP to disengage from one another. For SRβ, hydrolysis of GTP to trigger separation from SRα, subsequent nucleotide exchange, possibly catalyzed by the Sec61β subunit of the PCC (42), and reassociation with SRα for a new round of targeting are the necessary steps to be taken. In this cycle, SRβ could stay monomeric and toggle between a GTP- and GDP-bound state. However, SRβ dimerization and, therefore, silencing may be advantageous in situations where low secretory activity is desirable, as discussed above. A regulatory mechanism to empty SRβ and facilitate its dimerization would then populate a pool of silenced SRβ that might be used to quickly adjust to different levels of secretion.

The nucleotide-free SRβ structure is also an example for the caution one has to exercise when extrapolating protein function from seemingly very similar sequences. Here, the subtle differences to the Arf-type switch (43) suffice to create a quite different switch mode, likely to have three instead of just two switch positions. This structure now provides a framework for future biochemical studies addressing the regulation of cotranslational protein targeting.

Materials and Methods

Protein Purification and Crystallization. Production, purification, and crystallization of the protein used in the structural analysis were done as described in ref. 18. For *in vitro* experiments, expression constructs coding for nonpermuted SRβ domains [residues 31–244 from *S. cerevisiae* (scSRβ), 38–240 from *C. elegans* (ceSRβ), 60–266 from *Danio rerio* (drSRβ), and 59–271 from *H. sapiens* (hsSRβ)] tethered to a cleavable N-terminal His_6 tag were used. ScSRβ and hsSRβ constructs additionally encoded a C-terminal FLAG tag to increase solubility. SRβ was produced in BL21(DE3)RIL *E. coli* cells at 18°C or 30°C in LB medium. The protein was Ni-affinity-purified from the soluble cellular fraction and dialyzed against buffer A (10 mM potassium phosphate, pH 8.0/250 mM NaCl/1 mM DTT/0.5 mM EDTA), and the His_6 tag was cleaved. Further purification and removal of bound nucleotide was achieved by gel filtration on a Superdex S75 column (GE Healthcare) in buffer A. For microcalorimetric experiments, the gel filtration was performed in 10 mM potassium phosphate, pH 7.5, 250 mM NaCl, 0.5 mM Tris(2-carboxyethyl) phosphine (TCEP), and 0.5 mM EDTA. The monomeric, nucleotide-free SRβ elution fractions were concentrated and used in all experiments. The protein was at least 95% pure, as judged by SDS/PAGE analysis. SRα from *S. cerevisiae* was produced and purified as described in ref. 16.

Data collection, Structure Determination, and Refinement. A native data set to 2.2-Å resolution was collected at beamline X9A at the National Synchrotron Light Source at the Brookhaven Laboratory in Upton, NY (18). The structure was solved by using molecular replacement, with SRβ from the SRβ-GTP–SRX complex (PDB ID code 1NRJ) as the search model. Residues 61–101, the entire switch region, were removed from the search model to avoid model bias. Two solutions accounting for the two NCS-related cpSRβ molecules in the asymmetric unit were found with the program BEAST (44). The resulting solvent-flattened, NCS-averaged electron density map was of sufficient

quality to unambiguously build the cpSRβ-homodimer. Refinement was carried out with programs CNS (45) and REFMAC5 (44), model building with VUSETTE ZC (Mark Rould, personal communication) and COOT (46). The structure was refined to an R factor of 18.5% (R_{free} = 23.5%) by using data between 25 and 2.2 Å. Ramachandran plot analysis using MOLPROBITY (47) shows 314 residues in favored regions, six residues in allowed regions, and no outliers. The final model contains residues 36–64, 77–182, and 210–244 of monomer A, residues 37–59, 76–182, and 212–244 of monomer B, six sulfate ions, and 292 water molecules. The linker connecting S36 and L244 in the circularly permuted SRβ is not visible in either monomer.

***In Vitro* Dimerization Assay.** Generally, concentrated, nucleotide-free SRβ in buffer A was made 10 μM in 1 ml of buffer B (50 mM Tris·HCl, pH 8.5/250 mM NaCl/5 mM $MgCl_2$/1 mM DTT/0.25 mM EDTA) and incubated at 4°C. The pH of buffer B was varied from 7.7 to 9.1 to assay pH effect on dimerization. All pH values were measured at 4°C. GDP or GTP was added to buffer B to a final concentration of 1 mM to assay nucleotide effect on dimerization. After the indicated period, 250 μl was withdrawn and analyzed for dimer formation on a Superdex 75 10/300 GL column run at 4°C in 10 mM Tris·HCl, pH 8.5, 250 mM NaCl, 5 mM $MgCl_2$, 1 mM DTT, and 0.25 mM EDTA.

SRα-Binding Assays. To assay whether homodimeric SRβ binds SRα, nucleotide-free SRβ was incubated in buffer B for 6 days, and the resulting mixture of SRβ monomer and dimer was concentrated. This SRβ and SRα_{1-158} (SRX) were made at 10 μM each in 1 ml of 50 mM potassium phosphate, pH 7.5, 250 mM NaCl, 5 mM $MgCl_2$, 1 mM DTT, and 0.25 mM EDTA and incubated for 30 min. The reaction was then analyzed by gel filtration. SRβ-GTP–SRX heterodimer was prepared as described in ref. 16 and assayed by gel filtration for comparison.

Microcalorimetric Nucleotide Affinity Assay. The experiments were performed by using a MicroCal (Northhampton, MA) VP-ITC calorimeter. The protein solution was filtered and degassed by stirring under vacuum before use. Experiments were performed at 7°C. The sample cell was filled with 24.4 μM nucleotide-free, monomeric SRβ in an ITC buffer (10 mM potassium phosphate, pH 7.5/250 mM NaCl/0.5 mM Tris(2-carboxyethyl) phosphine/0.5 mM EDTA/5 mM $MgCl_2$). While being stirred at 310 rpm, the system was allowed to equilibrate before the start of the titration. The injection syringe was filled with a degassed solution of 450 μM FPLC-purified nucleotide (diluted at least 20-fold from a concentrated stock solution into ITC buffer), and repeated injections of 4 μl were made. Thermodynamic parameters N (stochiometry), K_A (association constant), and ΔH (enthalpy change) were obtained by nonlinear least-squares fitting of experimental data using a single-site binding model of the ORIGIN software package provided with the instrument. The free energy of binding (ΔG) and entropy change (ΔS) were obtained by using the equations $\Delta G = -RT \ln K_A$ and $\Delta G = \Delta H - T\Delta S$. The affinity of the nucleotide to SRβ is given as the dissociation constant ($K_D = 1/K_A$).

We thank R. Beckmann for critically reviewing this manuscript; R. Walczak for help with protein production and crystallization screening; J. S. Glavy, J. Helmers, and A. Hoelz for invaluable discussions; Debby Pheasant [Biophysical Instrumentation Facility, Massachusetts Institute of Technology (National Science Foundation Grant 0070319 and National Institutes of Health Grant GM68762)] for help with microcalorimetry; and the staff at beamline X9A (National Synchrotron Light Source, Brookhaven National Laboratory, Upton, NY) for help with data collection.

1. Keenan, R. J., Freymann, D. M., Stroud, R. M. & Walter, P. (2001) *Annu. Rev. Biochem.* **70,** 755–775.
2. Tajima, S., Lauffer, L., Rath, V. L. & Walter, P. (1986) *J. Cell Biol.* **103,** 1167–1178.
3. Gilmore, R., Walter, P. & Blobel, G. (1982) *J. Cell Biol.* **95,** 470–477.
4. Snapp, E. L., Reinhart, G. A., Bogert, B. A., Lippincott-Schwartz, J. & Hegde, R. S. (2004) *J. Cell Biol.* **164,** 997–1007.
5. Simon, S. M. & Blobel, G. (1991) *Cell* **65,** 371–380.
6. Van den Berg, B., Clemons, W. M., Jr., Collinson, I., Modis, Y., Hartmann, E., Harrison, S. C. & Rapoport, T. A. (2004) *Nature* **427,** 36–44.
7. Song, W., Raden, D., Mandon, E. C. & Gilmore, R. (2000) *Cell* **100,** 333–343.
8. Bacher, G., Pool, M. & Dobberstein, B. (1999) *J. Cell Biol.* **146,** 723–730.
9. Nagai, K., Oubridge, C., Kuglstatter, A., Menichelli, E., Isel, C. & Jovine, L. (2003) *EMBO J.* **22,** 3479–3485.
10. Doudna, J. A. & Batey, R. T. (2004) *Annu. Rev. Biochem.* **73,** 539–557.
11. Halic, M., Becker, T., Pool, M. R., Spahn, C. M., Grassucci, R. A., Frank, J. & Beckmann, R. (2004) *Nature* **427,** 808–814.
12. Egea, P. F., Shan, S. O., Napetschnig, J., Savage, D. F., Walter, P. & Stroud, R. M. (2004) *Nature* **427,** 215–221.
13. Focia, P. J., Shepotinovskaya, I. V., Seidler, J. A. & Freymann, D. M. (2004) *Science* **303,** 373–377.
14. Pool, M. R., Stumm, J., Fulga, T. A., Sinning, I. & Dobberstein, B. (2002) *Science* **297,** 1345–1348.
15. Miller, J. D., Tajima, S., Lauffer, L. & Walter, P. (1995) *J. Cell Biol.* **128,** 273–282.
16. Schwartz, T. & Blobel, G. (2003) *Cell* **112,** 793–803.
17. Ogg, S. C., Barz, W. P. & Walter, P. (1998) *J. Cell Biol.* **142,** 341–354.
18. Schwartz, T. U., Walczak, R. & Blobel, G. (2004) *Protein Sci.* **13,** 2814–2818.
19. John, J., Sohmen, R., Feuerstein, J., Linke, R., Wittinghofer, A. & Goody, R. S. (1990) *Biochemistry* **29,** 6058–6065.
20. Dreusicke, D. & Schulz, G. E. (1986) *FEBS Lett.* **208,** 301–304.
21. Chen, X., Court, D. L. & Ji, X. (1999) *Proc. Natl. Acad. Sci. USA* **96,** 8396–8401.
22. Scheffzek, K., Kabsch, W., Schlichting, I., Pai, E. F., Lautwein, A., Frech, M., Wittinghofer, A. & Goody, R. S. (1994) *Acta Crystallogr.* **50,** 521–526.
23. Londesborough, J. & Vuorio, O. E. (1993) *Eur. J. Biochem.* **216,** 841–848.
24. Liu, Y. & Eisenberg, D. (2002) *Protein Sci.* **11,** 1285–1299.
25. Rousseau, F., Schymkowitz, J. W. & Itzhaki, L. S. (2003) *Structure (London)* **11,** 243–251.
26. Mizuno, H., Fujimoto, Z., Koizumi, M., Kano, H., Atoda, H. & Morita, T. (1997) *Nat. Struct. Biol.* **4,** 438–441.
27. Limacher, A., Kloer, D. P., Fluckiger, S., Folkers, G., Crameri, R. & Scapozza, L. (2006) *Structure (London)* **14,** 185–195.
28. Bahadur, R. P., Chakrabarti, P., Rodier, F. & Janin, J. (2004) *J. Mol. Biol.* **336,** 943–955.
29. Legate, K. R. & Andrews, D. W. (2003) *J. Biol. Chem.* **278,** 27712–27720.
30. Pearson, M. A., Karplus, P. A., Dodge, R. W., Laity, J. H. & Scheraga, H. A. (1998) *Protein Sci.* **7,** 1255–1258.
31. Tweedy, N. B., Nair, S. K., Paterno, S. A., Fierke, C. A. & Christianson, D. W. (1993) *Biochemistry* **32,** 10944–10949.
32. Vetter, I. R. & Wittinghofer, A. (2001) *Science* **294,** 1299–1304.
33. Jekely, G. (2003) *BioEssays* **25,** 1129–1138.
34. Patil, C. & Walter, P. (2001) *Curr. Opin. Cell Biol.* **13,** 349–355.
35. Ma, Y. & Hendershot, L. M. (2001) *Cell* **107,** 827–830.
36. Schnell, D. J. & Hebert, D. N. (2003) *Cell* **112,** 491–505.
37. Weibel, P., Hiltbrunner, A., Brand, L. & Kessler, F. (2003) *J. Biol. Chem.* **278,** 37321–37329.
38. Sun, Y. J., Forouhar, F., Li Hm, H. M., Tu, S. L., Yeh, Y. H., Kao, S., Shr, H. L., Chou, C. C., Chen, C. & Hsiao, C. D. (2002) *Nat. Struct. Biol.* **9,** 95–100.
39. Andreotti, A. H. (2003) *Biochemistry* **42,** 9515–9524.
40. Schmid, F. X. (1993) *Annu. Rev. Biophys. Biomol. Struct.* **22,** 123–142.
41. Neuhard, J. & Nygaard, P. (1987) in *Escherichia coli and Salmonella typhimurium: Cellular and Molecular Biology*, ed. Neidhardt, F. C. (Am. Soc. Microbiol., Washington, DC), pp. 445–473.
42. Helmers, J., Schmidt, D., Glavy, J. S., Blobel, G. & Schwartz, T. (2003) *J. Biol. Chem.* **278,** 23686–23690.
43. Pasqualato, S., Menetrey, J., Franco, M. & Cherfils, J. (2001) *EMBO Rep.* **2,** 234–238.
44. Collaborative Computational Project 4 (CCP4), (1994) *Acta Crystallogr. D* **50,** 760–763.
45. Brunger, A. T., Adams, P. D., Clore, G. M., DeLano, W. L., Gros, P., Grosse-Kunstleve, R. W., Jiang, J. S., Kuszewski, J., Nilges, M., Pannu, N. S., *et al.* (1998) *Acta Crystallogr. D* **54,** 905–921.
46. Emsley, P. & Cowtan, K. (2004) *Acta Crystallogr. D* **60,** 2126–2132.
47. Lovell, S. C., Davis, I. W., Arendall, W. B., III, de Bakker, P. I., Word, J. M., Prisant, M. G., Richardson, J. S. & Richardson, D. C. (2003) *Proteins* **50,** 437–450.